Universal statistics of the scattering coefficient of chaotic microwave cavities

Sameer Hemmady,[1,2,3,4] Xing Zheng,[1,3] Thomas M. Antonsen, Jr.,[1,2,3] Edward Ott,[1,2,3] and Steven M. Anlage[1,2,4]
[1]*Department of Physics, University of Maryland, College Park, Maryland 20742, U.S.A.*
[2]*Department of Electrical and Computer Engineering, University of Maryland, College Park, Maryland 20742, U.S.A.*
[3]*Institute for Research in Electronics and Applied Physics, University of Maryland, College Park, Maryland 20742, U.S.A.*
[4]*Center for Superconductivity Research, University of Maryland, College Park, Maryland 20742, U.S.A.*
(Received 16 November 2004; published 31 May 2005)

We consider the statistics of the scattering coefficient S of a chaotic microwave cavity coupled to a single port. We remove the nonuniversal effects of the coupling from the experimental S data using the radiation impedance obtained directly from the experiments. We thus obtain the normalized scattering coefficient whose probability density function (PDF) is predicted to be universal in that it depends only on the loss (quality factor) of the cavity. We compare experimental PDFs of the normalized scattering coefficients with those obtained from random matrix theory (RMT), and find excellent agreement. The results apply to scattering measurements on any wave chaotic system.

DOI: 10.1103/PhysRevE.71.056215 PACS number(s): 05.45.Mt, 03.65.Nk, 11.55.−m, 03.50.De

I. INTRODUCTION

The scattering of short-wavelength waves by chaotic systems has motivated intense research activity, both theoretically and experimentally [1–3]. Some examples of wave chaotic systems include quantum dots [4], atomic nuclei [5], microwave cavities [2,6], and acoustic resonators [7]. Since these systems all have underlying chaotic ray dynamics, the wave pattern within the enclosure, as well as the response to external inputs, can be very sensitive to small changes in frequency and to small changes in the configuration. This motivates a statistical approach to the wave scattering problem [8].

The universal distribution for chaotic scattering matrices can be described by Dyson's circular ensemble [8–10]. However, the circular ensemble cannot typically be directly compared with experimental data because it applies only in the case of "ideal coupling" (which we define subsequently), while in experiments there are nonideal, system-specific effects due to the particular means of coupling between the scattering system (e.g., a microwave cavity) and the outside world. This nonuniversality of the raw experimental scattering data has long been appreciated and addressed in theoretical work [11–13]. Of particular note is the work of Mello, Peveyra, and Seligman (MPS), which introduces the distribution known as the Poisson kernel, where a scattering matrix $\langle S\rangle$ is used to parametrize the nonideal coupling. To apply this theory to an experiment, it is typically necessary to specify a procedure for determining a measured estimate of $\langle S\rangle$.

The first microwave experiments investigating scattering statistics by comparison with the theory of Refs. [11–13] were those of Ref. [15]. In analyzing their experimental data, Refs. [15,16] obtain an estimate for $\langle S\rangle$ by averaging measured S values over a number of different configurations of the cavity and over a suitable frequency range $[f_0-(1/2)\Delta f]$ to $[f_0+(1/2)\Delta f]$. We denote this experimentally obtained average as $\bar{S}$. For a given number of averaging configurations, the chosen frequency range must be large enough that good enough statistics is obtained, but at the same time be small enough that the variation of the coupling with frequency is not significant. To the extent that these conditions are satisfied, $\bar{S}$ will yield a good approximation to the desired $\langle S\rangle$. The quantity $\langle S\rangle$ in the theory describes direct (or prompt) processes [14] that depend only on the local geometry of the coupling ports, as opposed to complicated chaotic processes resulting from multiple reflections far removed from the coupling port. On the other hand, in obtaining $\bar{S}$, as in Refs. [15,16], averaging of the scattering data of the full chaotic system is employed. Thus, the data used to obtain $\bar{S}$ are the same measured data whose statistics is being studied. Also note that $\langle S\rangle$ is presumed to characterize the coupling, which is independent of the chaos of the system and is thus, in principle, a nonstatistical quantity. In this paper we shall pursue another approach [17]. Specifically, we seek to characterize the coupling in a manner that is both independent of the chaotic system and obtainable in a nonstatistical manner (i.e., without employing averages). As we explain in more detail subsequently, this latter point is of practical importance because of the inherent inaccuracy and sample size issues introduced by averaging a fluctuating quantity.

As discussed in Ref. [17], a direct means of investigating the statistics of typical chaotic scattering systems can be based on determination of the radiation impedance of the port Z_{rad} or equivalently $S_{rad'}$, the complex radiation scattering coefficient. The radiation scattering coefficient (respectively, radiation impedance) is the scattering coefficient (impedance) that would be observed if the distant boundaries of the cavity were made perfectly absorbing or moved to infinity. Therefore, it describes prompt processes at the port and can be shown to be equal to $\langle S\rangle$. The perfect coupling case corresponds to $S_{rad}=0$, in which all incident wave energy enters the cavity.

The radiation scattering coefficient S_{rad} can be directly measured in microwave experiments without resorting to averaging over a range of frequencies. Note that S_{rad} depends on the microwave frequency and thus, for the purposes of taking into account coupling, S_{rad} can be a more useful and

robust means of extracting universal properties from the data than $\overline{S}$, which depends on the frequency range Δf over which the averaging is done.

Another fundamental quantity characterizing coupling to the cavity is the impedance Z, which is related to S through the bilinear transformation

$$S = (Z + Z_o)^{-1}(Z - Z_o), \tag{1}$$

where Z_o is the characteristic impedance of the transmission line or waveguide feeding the port. The impedance linearly relates the voltage and the current phasors at the port and is determined solely by properties of the cavity and its port. In what follows we only discuss the one-port case; hence, Z and S are scalars (rather than matrices) throughout this paper. A more general discussion involving multiple ports can be found in Ref. [18]. Inverting the transformation Eq. (1), we can relate the radiation impedance $Z_{rad}=R_{rad}+iX_{rad}$ to the radiation scattering coefficient S_{rad} as

$$Z_{rad} = Z_o \frac{(1 + S_{rad})}{(1 - S_{rad})}. \tag{2}$$

In Refs. [17,19] it was shown that the cavity impedance Z can be expressed in terms of a scaled impedance z and the radiation impedance Z_{rad} as

$$Z = iX_{rad} + R_{rad}z, \tag{3}$$

where z is a complex random variable satisfying $\langle z\rangle = 1$. The random variable z has universal properties and describes the impedance fluctuations of a perfectly coupled cavity. The real part of z is well known in solid state physics as the local density of states (LDOS) and its statistics has been studied [20,21]. The imaginary part of z determines fluctuations in the cavity reactance. Discussion of the probability distribution of the normalized impedance z for microwave experiments has been presented in a previous paper [22].

The purpose of this paper is to study the universal statistical properties of the cavity scattering coefficient s defined in terms of the normalized impedance z

$$s = (z - 1)/(z + 1) = |s|e^{i\phi_s}, \tag{4}$$

which can be compared directly to theoretical predictions based on ideal coupling. Combining Eqs. (2)–(4), we obtain a formula relating s to the cavity scattering coefficient S and the cavity radiation scattering coefficient S_{rad}

$$s = \frac{(1 + S^*_{rad})}{(1 + S_{rad})} \frac{(S - S_{rad})}{(1 - SS^*_{rad})}. \tag{5}$$

The inverse of Eq. (5) giving the actual scattering amplitude S in terms of the normalized scattering amplitude s is a statement of the Poisson kernel [11,12] for a single-port cavity with internal loss. We note that the first factor in Eq. (5) is simply a phase shift which depends only on the coupling geometry. Thus, the magnitude of s satisfies

$$|s| = \left| \frac{S - S_{rad}}{1 - SS^*_{rad}} \right|. \tag{6}$$

According to the statistical theory, the only parameter on which the statistics of z and s depends is the loss due to the cavity wall absorption, which can be controlled and quantified in our experiment. We will experimentally verify the key theoretical predictions based on the circular ensemble hypothesis, such as the statistical independence of the magnitude and phase of the normalized scattering coefficient s, and the uniform probability distribution for the phase. Different degrees of loss and different coupling structures will be examined, and approximations to the probability density functions of s and z will be compared with the theoretical predictions from random matrix theory (RMT).

An expression similar to Eq. (6) was used by Kuhl *et al.* [16] to generate distributions of the scattering amplitudes S based on theoretical predictions for the normalized scattering amplitude s. Thus, it was assumed that the normalized scattering amplitude had the predicted properties of independence of magnitude and phase, and uniform distribution of phase. We will experimentally test these assumptions by using Eq. (5) directly to determine the properties of s.

Our paper is organized as follows. Section II presents our experimental setup and data collection. Section III carries out the normalization process to recover universal scattering characteristics and presents experimental histogram approximations to the probability density functions of the magnitude and phase of the normalized scattering coefficient s for different coupling structures and losses. Section IV explores a predicted relationship between the average cavity power reflection coefficient ($|S|^2$) and the magnitude of the radiation scattering coefficient. Section V discusses the advantages of employing the radiation scattering coefficient in uncovering universal properties, or of predicting raw scattering data. Section VI concludes the paper and gives the summary.

II. EXPERIMENTAL SETUP

Microwave cavities with irregular shapes (having chaotic ray dynamics) have proven to be very fruitful for the study of wave chaos, where not only the magnitude, but also the phase of scattering coefficients, can be directly measured from experiments. Our experimental setup consists of an air-filled quarter bow-tie chaotic cavity [Fig. 1(a)] which acts as a two-dimensional resonator below about 19 GHz [23]. Ray trajectories in a closed billiard of this shape are known to be chaotic. This cavity has previously been used for the successful study of the eigenvalue spacing statistics [6] and eigenfunction statistics [24,25] for a wave chaotic system. In order to investigate a scattering problem, we excite the cavity by means of a single coaxial probe whose exposed inner conductor, with a diameter ($2a$) extends from the top plate and makes electrical contact with the bottom plate of the cavity [Fig. 1(b)]. In this paper we study the properties of the cavity over a frequency range of 6–12 GHz, where the spacing between two adjacent resonances is on the order of 25–30 MHz.

As in the numerical experiments in Refs. [17,18], our experiment involves a two-step procedure. The first step is to collect an ensemble of cavity scattering coefficients S over the frequency range of interest. Ensemble averaging is real-

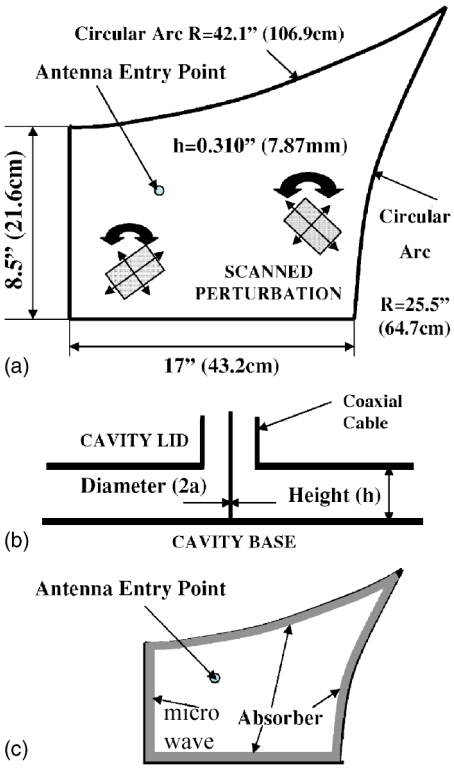

FIG. 1. (a) The physical dimensions of the quarter bow-tie chaotic microwave resonator are shown along with the position of the single coupling port. Two metallic perturbations are systematically scanned and rotated throughout the entire volume of the cavity to generate the cavity ensemble. (b) The details of the coupling port (antenna) and cavity height h are shown in cross section. (c) The implementation of the radiation case is shown, in which commercial microwave absorber is used to line the inner walls of the cavity to minimize reflections.

ized by using two rectangular metallic perturbations with dimensions $26.7\times40.6\times7.87$ mm^3 ($\sim$1% of the cavity volume), which are systematically scanned and rotated throughout the volume of the cavity [Fig. 1(a)]. Each configuration of the perturbers within the cavity volume results in a different value for the measured value of S. This is equivalent to measurements on cavities having the same volume, loss, and coupling geometry for the port, but with different shapes. The perturbers are kept far enough from the antenna so as not to alter its near-field characteristics. For each configuration, the scattering coefficient S is measured in 8000 equally spaced steps over a frequency range of 6–12 GHz. In total, 100 different configurations are measured, resulting in an ensemble of 800 000 S values. We refer to this step as the "cavity case."

The second step, referred to as the "radiation case," involves obtaining the scattering coefficient for the excitation port when waves enter the cavity but do not return to the port. In the experiment, this condition is realized by removing the perturbers and lining the side walls of the cavity with commercial microwave absorber (ARC Tech DD10017D) which provides about 25 dB of reflection loss between 6 and 12 GHz [Fig. 1(c)]. Note that the side walls of the cavity are outside the near-field zone of the antenna. Using the same frequency stepping of 8000 equally spaced points over 6–12 GHz, we measure the radiation scattering coefficient S_{rad} for the cavity. Such an approach approximates the situation where the side walls are moved to infinity; therefore, S_{rad} does not depend on the chaotic ray trajectories of the cavity, and thus gives a characterization of the coupling independent of the chaotic system. Reflecting the fact that the coupling aspects of the cavity typically vary over frequency, S_{rad} is usually frequency dependent.

Having measured the cavity S and S_{rad}, we then transform these quantities into the corresponding cavity and radiation impedances (Z and Z_{rad}), respectively, using Eqs. (1) and (2). The normalized impedance z is obtained by Eq. (3). In order to obtain z, every value of the determined cavity impedance Z is normalized by the corresponding value of Z_{rad} at the same frequency. The transformation in Eq. (4) [or equivalently, Eq. (5)] yields the normalized scattering coefficient $s=|s|\exp(i\phi_s)$, which is the key quantity of interest in this paper. Since the artifacts of nonideal coupling are supposed to have been "filtered out" through this normalization process, the statistics of the ensemble of s values should depend only on the net cavity loss.

In order to test the validity of the theory for systems with varying loss, we create different cavity cases with different degrees of loss. Loss is controlled and parametrized by placing 15.2-cm-long strips of microwave absorber along the inner walls of the cavity. These strips cover the side walls from the bottom to top lids of the cavity. We thus generate three different loss scenarios (loss case 0, loss case 1, loss case 3) [shown schematically in the insets to Fig 4(b)]. The numbers 0, 1, 3 correspond to the number of 15.2-cm-long strips placed along the inner cavity walls. The total perimeter of the cavity is 147.3 cm.

The theory predicts that, as long as the loss is the same, the normalized z or s will have the same statistical behavior. This prediction will be tested in our experiments with two different coupling geometries corresponding to coaxial cables with two different inner diameters [$2a=1.27$ mm and $2a=0.625$ mm, schematically shown in Fig. 1(b)].

III. EXPERIMENTAL RESULTS AND DATA ANALYSIS

In this section, we present our experimental findings for the statistical properties of the normalized scattering coefficient s, for different coupling geometries, and degrees of loss. This section is divided into three parts. In the first part, we give an example for the PDF of s at a specific degree of quantified loss and a certain coupling geometry. In the second part, we fix the degree of quantified loss, but vary the coupling by using coaxial cable antennas having inner conductors of different diameters ($2a=1.67$ mm and $2a=0.635$ mm). The PDF histograms for the magnitude and phase of s in these two cases will be compared. Finally, in the third part, we test the trend of the PDF of $|s|^2$ for a given coupling geometry and for three different degrees of quantified loss. Good agreement with random matrix theory is found in all cases.

A. Statistical independence of $|s|$ and ϕ_s

The first example we give is based on loss case 0 (i.e., no absorbing strips in the cavity) and coupling through a coaxial

cable with inner diameter $2a=1.27$ mm. Having obtained the normalized impedance z, we transform z into the normalized scattering coefficient s using Eq. (4). Since the walls of the cavity are not perfect conductors, the normalized scattering coefficient s is a complex scalar with modulus less than 1. (In loss case 0, most of the loss occurs in the top and bottom cavity plates since they have much larger area than the side walls.) Based on Dyson's circular ensemble, one of the most important properties of s is the statistical independence of the scattering phase ϕ_s and the magnitude $|s|$. Figure 2(a) shows a contour density plot of s in the frequency range of 6–9.6 GHz for loss case 0. The gray scale level at a given point in Fig. 2(a) indicates the number of points [for $\{\mathrm{Re}(s),\mathrm{Im}(s)\}$] that fall within a local rectangular region of size 0.02×0.02. We next arbitrarily take angular slices of this distribution that subtend an angle of $\pi/4$ radians at the center, and compute the histogram approximations to the PDF of $|s|$ using the points within those slices. The corresponding PDFs of $|s|$ for the three slices are shown in Fig. 2(b). We observe that these PDFs are essentially identical, independent of the angular slice. Figure 2(c) shows PDFs of ϕ_s computed for all the points that lie within two annuli defined by $0\leqslant|s|\leqslant0.3$ (stars) and $0.3<|s|\leqslant0.6$ (hexagons). These plots support the hypothesis that the magnitude of s is statistically independent of the phase ϕ_s of s, and that ϕ_s is uniformly distributed in 0 to 2π. This represents an experimental test of Dyson's circular ensemble hypothesis for wave chaotic scattering.

B. Detail independence of s

To further verify that the normalized s does not include any artifacts of system-specific, nonideal coupling, we take two identical wave chaotic cavities and change only the inner diameter of the coupling coaxial cable from $2a=1.27$ mm to $2a=0.635$ mm. Since the modification of the coaxial cable size barely changes the properties of the cavity, we assume that the loss parameters in these two cases are the same. The difference in the coupling geometry manifests itself as gross differences in the distribution of the raw cavity scattering coefficients S. This is clearly observable for the PDFs of the cavity power reflection coefficient $|S|^2$ as shown in Fig. 3(a) and the PDFs for the phase of S (denoted ϕ_S) shown in Fig. 3(c), for loss case 0 over a frequency range of 6–11.85 GHz. However, after measurement of the corresponding radiation impedance and the normalization procedure described above, we observe that the PDFs for the normalized power reflection coefficients are nearly identical, as shown in Fig. 3(b) for $|s|^2$ and the phase (ϕ_s) in Fig. 3(d). This supports the theoretical prediction that the normalized scattering coefficient s is a universal quantity whose statistics does not depend on the nature of the coupling antenna. Similarly, in Fig. 3(c), the phase ϕ_S of the cavity scattering coefficient S shows preference for certain angles. This is expected because of the nonideal coupling (impedance mismatch) that exists between the antenna and the transmission line. After normalization, the effects of nonideal coupling are removed and only the scattering phase of an ensemble of ideally coupled chaotic systems (in which all

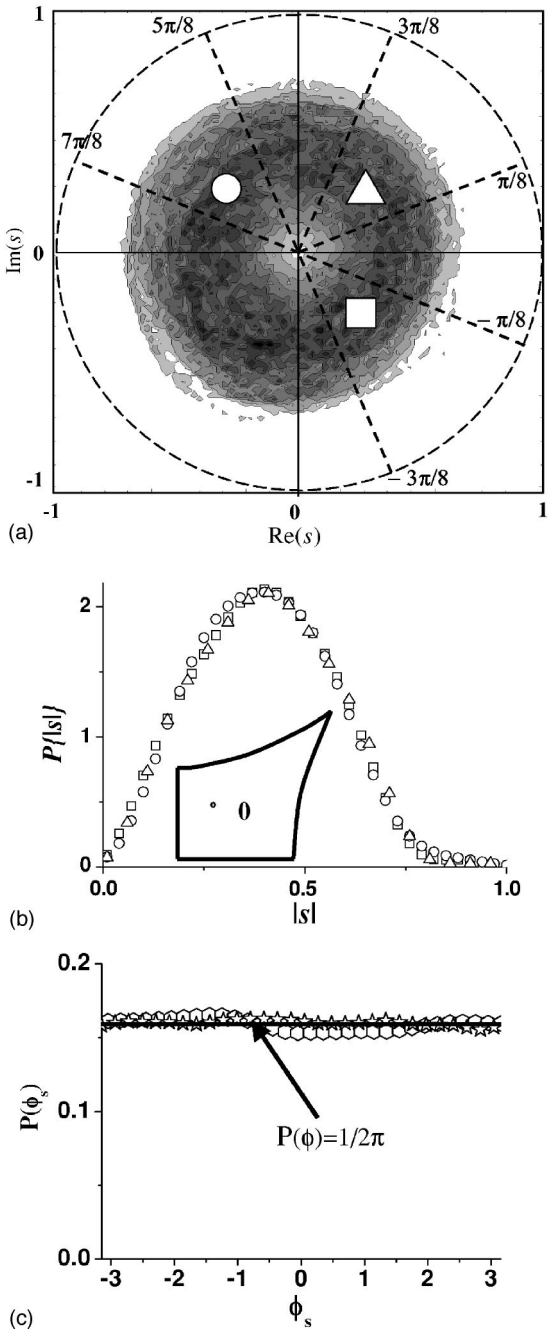

FIG. 2. (a) Polar contour density plot for the real and imaginary components of the normalized cavity s [$s=|s|\exp(i\phi_s)$] for loss case 0 in the frequency range of 6–9.6 GHz. The angular slices with the symbols (triangles, circles, squares) indicate the regions where the PDF of $|s|$ is calculated and shown in (b). Observe that the PDFs of the three regions are essentially identical. (c) The PDF of the phase ϕ_s of the normalized scattering coefficient s for two annuli defined by $0\leqslant|s|\leqslant0.3$ (stars) and $0.3<|s|\leqslant0.6$ (hexagons). Observe that these phase PDFs are nearly uniform in distribution. The uniform distribution is shown by the solid line [$P(\phi)=1/2\pi$]. This is consistent with the prediction that the $|s|$ is statistically independent of the phase ϕ_s of s.

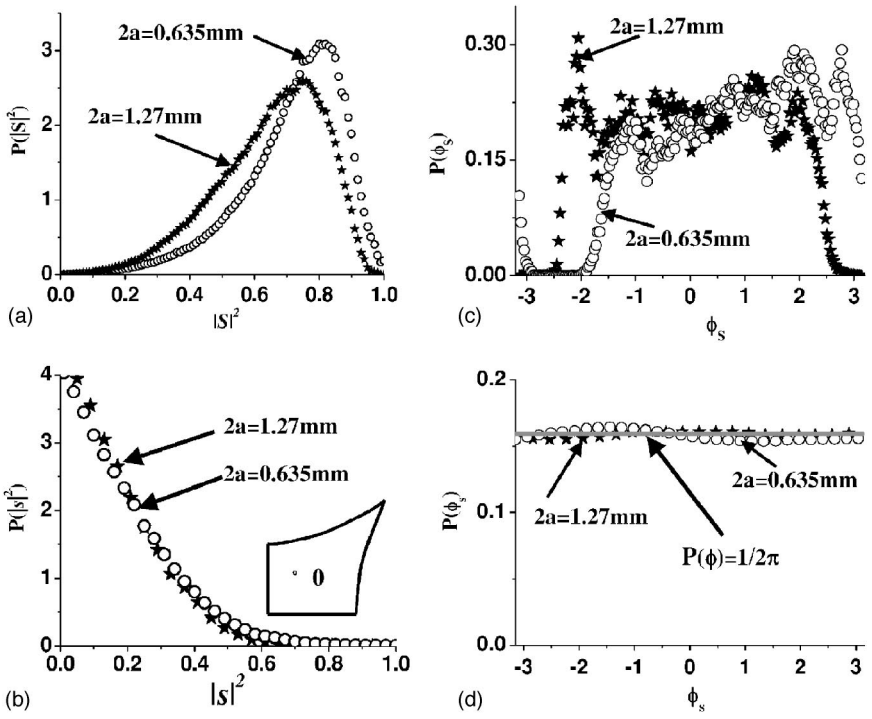

FIG. 3. (a) PDF for the un-normalized loss case 0 cavity $|S|^2$ in the frequency range of 6–11.85 GHz for two different coupling antenna diameters $2a=0.635$ mm (circles) and $2a=1.27$ mm (solid stars). (b) PDF for the normalized cavity $|s|^2$ in the frequency range of 6–11.85 GHz for two different coupling antenna diameters $2a=0.635$ mm (circles) and $2a=1.27$ mm (solid stars). Note that the disparities seen in (a) on account of the different coupling geometries disappear after normalization. (c) PDF for the un-normalized cavity phase (ϕ_S) for loss case 0 in the frequency range of 6–11.85 GHz for two different coupling antenna diameters $2a=0.635$ mm (circles) and $2a=1.27$ mm (solid stars). (d) PDF for the normalized cavity phase (ϕ_s) in the frequency range of 6–11.85 GHz for two different coupling antenna diameters $2a=0.635$ mm (circles) and $2a=1.27$ mm (solid stars). The normalized phase PDFs for the stars and circles in (d) are nearly uniformly distributed [the gray line in Fig. 4(d) shows a perfectly uniform distribution, $P(\phi)=1/2\pi$].

scattering phases are equally likely) is seen. Hence, consistent with theoretical expectations, the phase ϕ_s of normalized s data show an approximately uniform distribution [Fig. 3(d)].

C. Variation of *s* with loss

Having established that the coupling geometry is irrelevant for the distribution of s, we fix the coupling geometry (coaxial cable with inner diameter $2a=1.27$ mm) and vary the degree of quantified loss within the cavity. Three loss cases will be considered, namely, loss cases 0, 1, and 3. In Ref. [17] the degree of loss is characterized by a single damping parameter $\tilde{k}^2/Q$. Here, $\tilde{k}^2=k^2/\Delta k_n^2$, where $k=2\pi f/c$ is the wave number for the incoming frequency f and Δk_n^2 is the mean spacing of the adjacent eigenvalues k_n^2. The quantity Q is the quality factor of the cavity. The parameter $\tilde{k}^2/Q$ represents the ratio of the frequency width of the cavity resonances due to distributed losses, and the average spacing between resonant frequencies.

For sufficiently high loss, the variances (σ^2) of the PDFs of the real and imaginary parts of z can be related to $\tilde{k}^2/Q$ by [17]

$$\sigma^2_{\mathrm{Re}(z)} = \sigma^2_{\mathrm{Im}(z)} = Q/(\pi \tilde{k}^2). \tag{7}$$

This relation has been experimentally validated for different cavities and for different coupling geometries [22]. Thus, we can determine the damping parameter from measuring the variance of the PDFs of the real or imaginary part of z (such as those shown in Fig. 4). With this parameter determined, we use a Monte Carlo simulation based on random matrix theory [see Eq. (29) of Ref. [17] and the discussion therein] to calculate the theoretically predicted PDFs of z and s. (Approximate formulas for the PDFs of Re[z] [20] and Im[z] [26], which agree well with the Monte Carlo results, are also available.) The solid curves in Fig. 4 are plots from RMT for values of $\tilde{k}^2/Q$ that are obtained by computing the variances, while the symbols are obtained from histogram approximations to the PDFs of the normalized impedance z extracted from the experimental data over a frequency range of 6.5–7.8 GHz. Generally, as the loss of the cavity increases, the PDF of the normalized imaginary part of the impedance loses its long tails and begins to sharpen up, developing a Gaussian appearance [Fig. 4(b)]. At the same time, the PDF of the normalized real part smoothly evolves from being peaked between $\mathrm{Re}(z)=0$ and $\mathrm{Re}(z)=1$, into a Gaussian-type distribution that peaks at $\mathrm{Re}(z)=1$ [Fig. 4(a)].

The symbols in Fig. 5 (presented on a semilogarithmic scale) show the PDF of the normalized power reflection coefficient ($r=|s|^2$) in the frequency range 6.5–7.8 GHz for three different loss cases. The solid lines are the predictions for the PDF of r, $P(r)$ for different values of the loss parameter $\tilde{k}^2/Q$. In Fig. 5, the $\tilde{k}^2/Q$ parameters are the same as those for Fig. 4, and were obtained from the variances of the

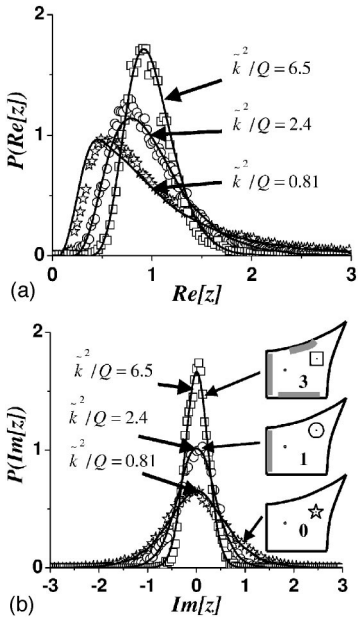

FIG. 4. PDFs for the (a) real and (b) imaginary parts of the normalized cavity impedance z for a wave chaotic microwave cavity between 6.5 and 7.8 GHz with $h=7.87$ mm and $2a=1.27$ mm, for three values of loss in the cavity (open stars: 0, circles: 1, squares: 3 strips of absorber). Also shown are single parameter, simultaneous fits for both PDFs (solid curves), where the loss parameter $\tilde{k}^2/Q$ is obtained from the variance of the data in (a) and (b).

PDFs of the real or imaginary parts of z. We observe that our data conform well to the predictions from random matrix theory for all degrees of loss.

IV. RELATIONSHIP BETWEEN CAVITY AND RADIATION POWER REFLECTION COEFFICIENTS

As a final experimental test, we would like to examine how the measured cavity power reflection coefficient depends only on the radiation scattering coefficient and losses

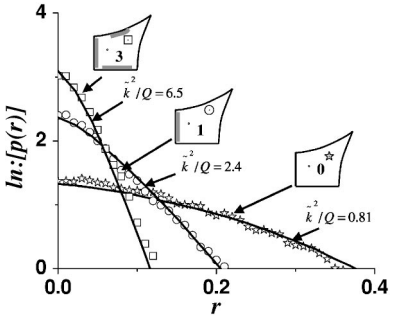

FIG. 5. PDF for the normalized power reflection coefficient $r=|s|^2$ on a natural log scale for loss case 0, 1, 3 (stars, circles, and squares, respectively) in the frequency range of 6.5–7.8 GHz. These are from the same data as used to obtain Fig. 4. Also shown is the prediction of the model in Ref. [17] (solid lines) for $P(r)$ using the values of $\tilde{k}^2/Q$ obtained from the variances of the distributions in Fig. 4.

in the cavity. Reference [18] predicts that the average value of the cavity power reflection coefficient $\overline{|S|^2}$ depends only on the magnitude of the radiation scattering coefficient ($|S_{rad}|$) and the loss parameter $\tilde{k}^2/Q$, and is independent of the phase of S_{rad}. The quantity $|S_{rad}|$ is related to the radiation impedance ($Z_{rad}=R_{rad}+iX_{rad}$) through the transformation

$$|S_{rad}| = \sqrt{\frac{(R_{rad}-Z_o)^2+(X_{rad})^2}{(R_{rad}+Z_o)^2+(X_{rad})^2}}. \tag{8}$$

We consider a cavity having quantified loss (loss Cases 0, 1, and 3), with a coupling port of diameter $2a=1.27$ mm and over the frequency range of 6.5–7.8 GHz. Having experimentally generated the normalized z as described above, we then simulate an ensemble of similar cavities but with different coupling "geometries." This is done by means of a lossless two-port impedance transformation [18] of our z data, as described by the relation

$$z' = \frac{1}{(1/z + i\beta)}, \tag{9}$$

which corresponds to adding a reactive impedance $-i/\beta$ in parallel with the impedance z.

The quantity z' thus simulates the impedance of a hypothetical cavity that is non-ideally coupled to the excitation port, and the coupling geometry is characterized by the real factor β, which can be varied in a controlled manner. We also define a transformed radiation impedance (z'_{rad}) given by

$$z'_{rad} = \frac{1}{(1+i\beta)}. \tag{10}$$

For the generation of z'_{rad}, the factor β is varied over the same range of values as used to generate z'. Having determined z' and its corresponding z'_{rad}, we determine the scattering coefficients s' and s'_{rad} through the transformations

$$s' = (z'-1)/(z'+1), \tag{11}$$

$$s'_{rad} = (z'_{rad}-1)/(z'_{rad}+1). \tag{12}$$

A range of β values is chosen to cover all possible coupling scenarios. We then plot the average of $|s'|^2$ (i.e., $\overline{|s'|^2}$) as a function of s'_{rad}. This approach is followed for all three loss cases (loss cases 0, 1, and 3) resulting in the data sets with star, circles, and squares, respectively, in Fig. 6. First note that all curves originate from the point $\overline{|s'|^2}=|s'_{rad}|=1$, which may be thought of as the perfectly *mis*matched case. Next, consider $|s'_{rad}|<1$, and observe that as the losses increase, the curves shift downwards for a fixed coupling (characterized by $|s'_{rad}|$). This is intuitively reasonable because, as the absorption (losses) within the cavity increases, we expect less signal to return to the antenna (i.e., smaller $\overline{|s'|}$) for a given coupling $|s'_{rad}|$. From the variance of the PDF of Re[z] for the above loss cases, we determine $\tilde{k}^2/Q$ to be 0.81, 2.4, and 6.5 for loss cases 0, 1, and 3, respectively. The solid lines in Fig. 6 are obtained from the RMT theoretical predictions for the perfectly coupled scattering coefficient s with the appropriate values for $\tilde{k}^2/Q$. Next, these are transformed using Eqs. (9) and (10) with the same range of coupling factors (β) as used

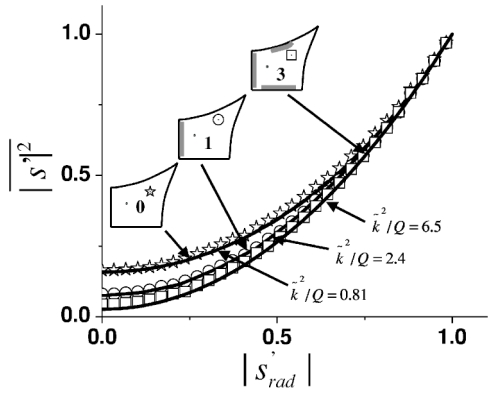

FIG. 6. Dependence of the average of the cavity power reflection coefficient $\overline{|s'|^2}$ on the magnitude of the radiation scattering coefficient $|s'_{rad}|$, for different loss cases (loss case 0: stars; loss case 1: circles; loss case 3: squares). The data are shown for the frequency range of 6.5–7.8 GHz. Also shown are the numerical simulations from the RMT based upon the $\tilde{k}^2/Q$ values 0.81, 2.4 and 6.5 for loss cases 0, 1, and 3, respectively (solid lines).

for the experimentally determined z'. We observe good agreement between the numerical simulations from RMT (solid lines in Fig. 6) and our experimentally derived points.

For a given lossy cavity one can also consider its lossless N-port equivalent. By the lossless N-port equivalent we mean that the effect of the losses distributed in the walls of our cavity can be approximated by a lossless cavity with $N-1$ extra perfectly coupled (pc) ports through which power coupled into the cavity can leave. The point $|S_{rad}|=|s'_{rad}|=0$ in Fig. 6 corresponds to perfect coupling. In this case, Ref. [18] predicts that the vertical axis intercept of these curves corresponds to the lossless N-port equivalent of the distributed losses within the cavity; i.e., at $|s'_{rad}|=0$ we have $\overline{|s'|^2}|_{pc}=2/(N+1)$ (for time-reversal symmetric wave chaotic systems). Thus, in our experiment the quantified loss in loss cases 0, 1, and 3 is equivalent to ~11, 24, and 45 perfectly coupled ports, respectively. In other words, for all intents and purposes, the cavity can be considered lossless but perfectly coupled to this number of ports.

V. VALIDATING THE USE OF RADIATION IMPEDANCE TO CHARACTERIZE NONIDEAL COUPLING

In sec. III we used the radiation impedance (Z_{rad}), or the radiation scattering coefficient (S_{rad}), as a tool to characterize the non-ideal coupling (direct processes) between the antenna and the cavity. This quantity is measurable and is only dependent on the local geometry around the port. As previously noted, Refs. [15,16] use configuration and frequency averaged scattering data to obtain an approximation to $\langle S\rangle$. For a given center frequency f_0, this procedure relies on the satisfaction of two requirements: first, the range of Δf must be large enough to include a large number of modes; second, S_{rad} must vary little over the range of Δf.

The nature of the variation of S with frequency is illustrated in Fig. 7, where a plot $[\mathrm{Re}(S),\mathrm{Im}(S)]$ of the complex scattering coefficient for a cavity in the frequency range of

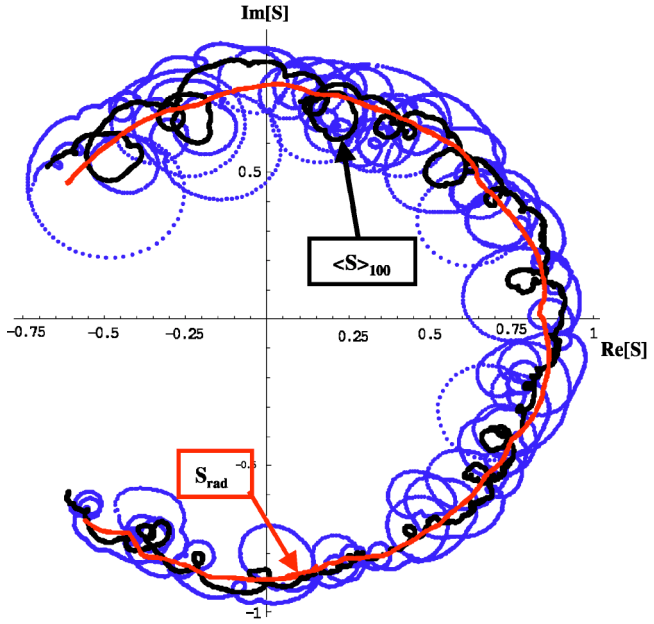

FIG. 7. (Color online) Polar plot for the cavity scattering coefficient $S=\mathrm{Re}(S)+i\,\mathrm{Im}(S)$ is shown for a frequency range of 6–12 GHz for loss case 0 and with a coupling port of diameter $2a=1.27$ mm. The blue trace represents one single rendition of the cavity for a selected position and orientation of the perturbers. Each circular loop represents an isolated resonance. The black trace is the ensemble average $\langle S\rangle_{100}$ over 100 different locations and orientations of the perturbers within the cavity. The meandering nature of the black trace shows that remnants of the cavity resonances are still present because of the finite number of ensemble averages. The red trace shows the radiation scattering coefficient for the same port. This trace is smooth because the radiation scattering coefficient approximates the cavity boundaries being extended to infinity.

6–12 GHz is shown. The blue trace shows results for S for a single configuration of the cavity corresponding to a given position and orientation of the perturbers [Fig. 1(a)]. Isolated resonances are seen as circular loops in the polar plot. The degree of coupling is indicated by the diameter of the loops. Frequency ranges where the coupling is good would manifest themselves as large loops, while those frequency ranges with poor coupling result in smaller loops. Ensemble averaging 100 such different configurations of this cavity for different positions and orientations of the perturber produces the black trace denoted as $\langle S\rangle_{100}$. Note that even with 100 cavity renditions, the fluctuations in $\langle S\rangle_{100}$ are still present and are seen as the meanders in the black trace. The red trace, which corresponds to the radiation scattering coefficient for this antenna geometry, is devoid of such fluctuations (because there are no reflected waves from the far walls back to the port) and is easily obtainable in practice without resorting to generating large ensemble sets of cavity configurations. Moreover, since the radiation impedance of the port is also a function of frequency, there is no constraint on the frequency span where the analysis for obtaining the universal statistics of s (or z) can be carried out.

To quantitatively illustrate this point, we recover the nonuniversal scattering statistics of a given cavity for a given type of coupling using only the measured radiation imped-

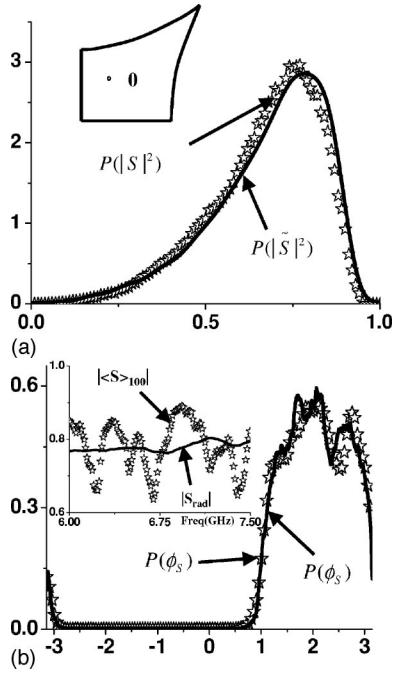

FIG. 8. (a) The experimental PDF for the loss case 0 cavity power reflection coefficient ($|S|^2$) (stars) over a frequency range of 6–7.5 GHz. Also shown is the numerical estimate $P(|\tilde{S}|^2)$ (solid trace) determined from RMT and the experimentally measured radiation impedance of the port (Z_{rad}). (b) The experimental PDF for the loss case 0 cavity scattering phase (ϕ_s) (stars) over a frequency range of 6–7.5 GHz. Also shown is the numerical estimate P($\phi_{\tilde{S}}$) (solid trace) determined from RMT and the experimentally measured radiation impedance of the port. We observe good agreement between the measured data and the numerically estimated PDFs. The inset shows the fluctuation in $|\langle S\rangle_{100}|$ (stars) over the frequency range of 6–7.5 GHz, while the solid trace shows the magnitude of the experimentally measured radiation scattering coefficient ($|S_{rad}|$).

ance of the coupling port and the numerically generated normalized impedance z from RMT, which depends only upon the net losses within the cavity. We consider a loss case 0 cavity, over a frequency range of 6–7.5 GHz, which is excited by means of a coaxial cable of inner diameter ($2a$ = 1.27 mm). The variation in $|\langle S\rangle_{100}|$ [inset of Fig. 8(b)] apparently indicates that the coupling characteristics for this setup fluctuate over the given frequency range, undergoing roughly four or five oscillations over a range in $|\langle S\rangle_{100}|$ of order 0.2. Thus, the frequency-averaged $|\langle S\rangle_{100}|$ would be expected to be an unreliable estimate to parametrize the coupling over this frequency range.

We can estimate the parameter $\tilde{k}^2/Q$ using the center frequency (k=141.3 m^{-1}), the average spacing between eigenmodes for our cavity (Δk_n^2=109.2 m^{-2}) [22], and typical Q values of ($Q\sim 225$), yielding an estimated $\tilde{k}^2/Q$=0.8. We use this parameter to generate an ensemble of $s(\omega)$ following Ref. [17] and Eq. (4), combine it with the measured $S_{rad}(\omega)$ of the antenna, and employ Eq. (5) to obtain an estimate of the nonuniversal system-specific scattering coefficient, which we denote as $\tilde{S}$.

In Fig. 8(a), the PDF of $|\tilde{S}|^2$ is shown as the solid trace, while the experimentally measured PDF of $|S|^2$ is shown as the stars. In Fig. 8(b), the PDF of $\phi_{\tilde{S}}$ is shown as the solid trace with experimentally measured PDF of ϕ_S shown as the stars. We observe good agreement between the numerically generated estimate and the actual data. This result validates the use of the radiation impedance (scattering coefficient) to accurately parametrize the system-specific, nonideal coupling of the ports, and also provides us with a way to predict beforehand the statistical properties of other complicated enclosures nonideally coupled to external ports.

VI. CONCLUSIONS

The results discussed in this paper serve to establish a solid ground that can be used to extract universal statistical properties from data on wave chaotic systems, or to engineer wave chaotic cavities with specific statistical transport properties. In addition, given the frequency, volume, and amount of losses (parametrized by Q) within the enclosure, and the radiation impedance of the ports, Refs. [17,18] provide us with a tool to predict the statistics of the cavity response (Z and S) *a priori*.

We have shown that a simple normalization based on the radiation impedance can be used to remove nonuniversal, system-specific coupling details and bring out the universality in the measured impedance and scattering statistics of wave chaotic systems. This normalization procedure has allowed us to experimentally verify theoretical predictions for the universal properties of a one-port wave chaotic system. We have also tested several aspects of the theory in the realm of intermediate to high loss and for different coupling geometries, and find good agreement with theoretical predictions. We have shown that the average of the cavity power reflection coefficient $\overline{|S|^2}$ depends only on the magnitude of the radiation scattering coefficient $|S_{rad}|$ and the degree of loss, and have obtained good agreement between theory and experiments. Finally, we also demonstrate the ability of this normalization procedure to faithfully reproduce the nonuniversal statistics of the scattering coefficient phase and magnitude of chaotic cavities when $|\langle S\rangle|$ is not constant over the frequency range examined. These results should not be regarded as limited to microwave cavities or any specific coupling structure, but as applying to any wave chaotic system coupled to the outside world.

ACKNOWLEDGMENTS

We acknowledge useful discussions with R. Prange and S. Fishman, as well as comments from Y. Fyodorov, D.V. Savin, and P. Brouwer. This work was supported by the DOD MURI for the study of microwave effects under AFOSR Grant F496200110374 and AFOSR DURIP Grant FA95500410295.

[1] F. Haake, *Quantum Signatures of Chaos* (Springer-Verlag, Berlin, 1991).
[2] H.-J. Stockmann, *Quantum Chaos* (Cambridge University Press, Cambridge 1999), and references therein.
[3] R. Holland and R. St. John, *Statistical Electromagnetics* (Taylor and Francis, London, 1999), and references therein.
[4] Y. Alhassid, Rev. Mod. Phys. **72**, 895 (2000).
[5] R. U. Haq, A. Pandey, and O. Bohigas, Phys. Rev. Lett. **48**, 1086 (1982).
[6] P. So, S. M. Anlage, E. Ott, and R. N. Oerter, Phys. Rev. Lett. **74**, 2662 (1994).
[7] O. I. Lobkis, I. Rozhkov, and R. Weaver, Phys. Rev. Lett. **91**, 194101 (2003).
[8] E. P. Wigner, Ann. Math. **53**, 36 (1951); **62**, 548 (1955); **65**, 203 (1957); **67**, 325 (1958).
[9] F. J. Dyson, J. Math. Phys. **3**, 140 (1962).
[10] M. L. Mehta, *Random Matrices* (Academic Press, San Diego, 1991).
[11] P. A. Mello, P. Peveyra, and T. H. Selgiman, Ann. Phys. **161**, 254 (1985).
[12] P. W. Brouwer, Phys. Rev. B **51**, 16878 (1995).
[13] D. V. Savin, Y. V. Fyodorov, and H.-J. Sommers, Phys. Rev. E **63**, 035202 (2001).
[14] E. Kogan, P. A. Mello, and H. Liqun, Phys. Rev. E **61**, R17 (2000).
[15] R. A. Mendez-Sanchez, U. Kuhl, M. Barth, C. H. Lewenkopf, and H.-J. Stockmann, Phys. Rev. Lett. **91**, 174102 (2003).
[16] U. Kuhl, M. Martinez-Mares, R. A. Mendez-Sanchez, and H.-J. Stockmann, Phys. Rev. Lett. **94**, 144101 (2005).
[17] X. Zheng, T. M. Antonsen, and E. Ott, e-print cond-mat/0408327 J. Electromag. (to be published).
[18] X. Zheng, T. M. Antonsen, and E. Ott, e-print cond-mat/0408317 J. Electromag. (to be published).
[19] L. K. Warne, K. S. H. Lee, H. G. Hudson, W. A. Johnson, R. E. Jorgenson, and S. L. Stronach, J. Inst. Math. Appl. **51**, 978 (2003).
[20] K. B. Efetov and V. N. Prigodin, Phys. Rev. Lett. **70**, 1315 (1993).
[21] C. W. J. Beenakker, Phys. Rev. B **50**, 15170 (1994).
[22] S. Hemmady, X. Zheng, E. Ott, T. Antonsen, and S. M. Anlage, Phys. Rev. Lett. **94**, 014102 (2005).
[23] Ali Gokirmak, Dong-Ho Wu, J. S. A. Bridgewater, and Steven M. Anlage, Rev. Sci. Instrum. **69**, 3410 (1998).
[24] D.-H. Wu, J. S. A. Bridgewater, A. Gokirmak, and S. M. Anlage, Phys. Rev. Lett. **81**, 2890 (1998).
[25] S.-H. Chung, A. Gokirmak, D.-H. Wu, J. S. A. Bridgewater, E. Ott, T. M. Antonsen, and S. M. Anlage, Phys. Rev. Lett. **85**, 2482 (2000).
[26] Y. Fyodorov and D. V. Savin, JETP **80**, 725 (2004); Pis'ma Zh. Eksp. Teor. Fiz. **80**, 855 (2004).